9th AIAA Flow Control Conference, 25–29 June 2018, Atlanta, Georgia.

2018-3690

Reduced-Order Models for
Feedback Control of Transient Energy Growth

Aniketh Kalur* and Maziar S. Hemati†

Aerospace Engineering and Mechanics, University of Minnesota, Minneapolis, MN 55455, USA.

Feedback flow control is developed to suppress the transient energy growth of flow disturbances in a linearized channel flow. Specifically, we seek a controller that minimizes the maximum transient energy growth, which can be formulated as a linear matrix inequality problem. Solving linear matrix inequality problems can be computationally prohibitive for high-dimensional systems encountered in flow control applications. Thus, we develop reduced-order fluids models using balance truncation and proper orthogonal decomposition techniques. These models are designed to optimally approximate system energy while preserving the input-output dynamics that are essential for controller synthesis. Controllers developed based on these reduced-order models are found to reduce transient energy growth and to outperform linear quadratic controllers in the context of a linearized channel flow.

I.   Introduction

In a wide sense, flow control is the manipulation of a fluid flow by passive or active means in order to achieve a beneficial result [1]. Flow control is a burgeoning field of fluid dynamics where modern control methodologies are applied to fluid systems to regulate, suppress, and control undesirable mechanisms that lead to flow instabilities that degrade performance. Of particular interest in the current study is to use feedback flow control to suppress flow instabilities that transition a flow from a low-drag laminar state to a high-drag turbulent state. Laminar to turbulent transition in shear flow often arises at a Reynolds number (Re) well below the critical Re determined from a linear stability analysis of the Navier-Stokes equations about a laminar equilibrium profile [2]. Extensive studies have suggested that sub-critical transition arises as a result of non-modal mechanisms for transient energy growth (TEG) of flow disturbances [2–5, 25]. In turn, numerous studies have sought to delay transition by reducing TEG through the implementation of passive and active control strategies. This paper predominantly deals with the reduction of TEG using modern feedback control theory, as discussed in future sections.

Active flow control via feedback is able to modify the natural dynamics of the system, and so can be used to reduce TEG and delay transition. Indeed, numerous investigations have sought to reduce TEG and delay transition using classical and modern feedback control techniques [6–10, 12]. Linear quadratic optimal control synthesis has been a prominent control approach in many transition delay investigations and has been successfully demonstrated for a number of flow control applications. However, linear quadratic optimal control techniques may not be the most natural choice for TEG reduction. Linear quadratic control techniques are optimal in the sense that they minimize the balance of the integrated perturbation and input energies over some time horizon; although experience suggests that linear quadratic designs can be tuned to reduce TEG, there are no guarantees that controllers that aim to minimize integrated energies will minimize—or even reduce—TEG. Rather than designing controllers in this standard manner, it seems more appropriate to design optimal controllers that explicitly include TEG reduction in the objective function. Indeed, a more suitable control objective for TEG reduction would be to minimize the maximum TEG, as proposed by Whidborne and colleagues [11, 13]. The maximum TEG is the peak energy that arises from a worst-case or optimal disturbance [3]; thus, minimizing the maximum TEG ensures that TEG will be reduced

---

*Graduate Student and AIAA Member.
†Assistant Professor and AIAA Senior Member.

from all disturbances. The associated controller synthesis problem for minimizing the maximum TEG can be recast as a linear matrix inequality (LMI), which can be solved using numerical methods developed in the optimization community (e.g., interior-point methods [14]). However, the associated LMI problems tend to be computationally demanding for the high-dimensional systems encountered in flow control applications; indeed, the memory demands of such methods scale as $\mathcal{O}(n^6)$, where n is the state dimension [13].

One approach to overcoming the computational challenge of LMI-based controller synthesis is through the use of model reduction techniques [23, 24]. Indeed, reduced-order models (ROMs) have been leveraged in a number of flow control applications, including the use of global mode truncation for LMI-based synthesis in channel flow [13]. Global modes capture physically relevant flow structures that contribute to TEG, making the approach natural for model reduction. Moreover, global modes can easily be used to reconstruct the full state of the system, and can thus be used to approximate the physical energy of the system—an important consideration for TEG studies. However, despite their physical relevance and convenience, ROMs based on global modes are not necessarily the best choice for controller synthesis in the context of TEG. Global modes are not the optimal basis for capturing the energy of the system—proper orthogonal decomposition (POD) is optimal for approximating system energy. Nor are global modes optimal for capturing the input-output dynamics of the system—balanced truncation (BT) is optimal for approximating input-output dynamics.

In the present study, we advocate for a combined POD-BT approach (i.e., balanced truncation with output projection [16]). for arriving at suitable control-oriented ROMs for TEG reduction. Specifically, we propose to project the full-state output onto a reduced basis of POD modes, in order to optimally approximate the physical energy of the system—a quantity that must be faithfully captured for TEG reduction. We then leverage the balanced truncation technique to optimally capture the input-output dynamics of the system— i.e., the dynamics from control inputs to POD coefficients. In the event that balanced truncation cannot be performed directly, then the balanced POD method can be used instead [16]. The results of this study indicate that this approach can reliably generate low-order fluids models that make LMI-based controller synthesis tractable and effective at minimizing the maximum TEG on the full-order fluids system.

This paper is organized as follows: Section II is categorized into two sub-sections, where subsection II.A provides a brief introduction to the LQR and LMI control synthesis methods. The subsection II.B details the reduced-order modeling framework developed for fluid flows. We begin section III, by briefly describing the linearized channel flow model used for reduced-order modeling and controller synthesis in this paper. In subsection III.A we study the performance of the reduced-order models with respect to the full-order model. The subsection III.B discusses the performance of controllers in suppressing TEG, the controllers are developed using the reduced-order modeling framework introduced in this paper. Section IV draws conclusions on the performance of the reduced-order models and controllers.

II.   Reduced-Order Modeling and Controller Design

II.A.   Controller Synthesis

Consider the linearization of the Navier-Stokes equations about a laminar equilibrium profile,

$$\dot{\mathbf{x}}(t) = A\mathbf{x}(t) + B\mathbf{u}(t) \tag{1}$$

where $\mathbf{x}(t) \in \mathbb{R}^n$ is the state vector, $\mathbf{u}(t) \in \mathbb{R}^p$ is the input vector, and $t \in \mathbb{R}$ is time. The perturbation energy as a function of time is then given by,

$$E(t) = \mathbf{x}^T(t) \, Q \, \mathbf{x}(t), \ t \geq 0 \tag{2}$$

where $Q = Q^T > 0$ is a weighting matrix. The maximum TEG (Θ) is defined as,

$$\Theta = \max_{t \geq t_0} \max_{E(t_0) \neq 0} \frac{E(t)}{E(t_0)}, \tag{3}$$

which results from a so-called *worst-case* or *optimal disturbance* [3].

Linear quadratic optimal control has been studied extensively for TEG reduction and transition delay [12, 13, 17]. The linear quadratic regulator (LQR) problem aims to find the control input that minimizes the

integrated balance of state and input energy,

$$\min_{\mathbf{u}(t)} J = \int_0^\infty (\mathbf{x}^T Q \mathbf{x} + \mathbf{u}^T R \mathbf{u}) dt \tag{4}$$

subject to the linear dynamic constraint in (1) and $R > 0$.

As we have already discussed, LQR control is not guaranteed to minimize or even reduce TEG. Here, we instead follow the approach of [11, 13], and aim to find a feedback law that minimizes the maximum TEG, Θ. A detailed derivation and description of the synthesis approach can be found in [11]. Here, we only present highlights of the approach. To simplify our presentation here, we take $Q = I$. Note this is done without loss of generality since the state can always be transformed as $\hat{\mathbf{x}}(t) = Q^{1/2}\mathbf{x}(t)$ to satisfy this condition. Then, a feedback control law that minimizes the upper bound Θ_u of the maximum TEG can be determined from the solution to the LMI generalized eigenvalue problem [11]:

$$\min \gamma$$
$$\text{subject to} \quad I \leq P \leq \gamma I$$
$$P = P^T > 0 \tag{5}$$
$$AP + PA^T + BY + Y^T B^T < 0$$

Here, γ upper bounds Θ_u, and so minimizing γ minimizes the maximum TEG. The resulting full-state feedback control law is given by $\mathbf{u}(t) = YP^{-1}\mathbf{x}(t)$. The LMI problem in (5) can be solved by standard techniques [14]; however, these standard algorithms can be computationally demanding, with memory requirements scaling as $\mathcal{O}(n^6)$, where n is the state dimension [13]. This is a prohibitive property of the LMI formulation for high-dimensional systems, such as fluid flows. In the next section, we discuss an approach for generating reduced-order models that can make these computations tractable for many applications, while still yielding controllers that perform well on the full-order system.

II.B. Control-Oriented Reduced-Order Modeling

The development of LMI-based controllers becomes challenging in the context of the high-dimensional systems of interest in flow control applications. In this section, we outline an approach for model reduction that will be suitable for LMI-based synthesis aimed at minimizing the maximum TEG, described above. Since the notion of energy is central to TEG, it will be important to faithfully capture the system energy with the resulting reduced-order model (ROM). Further, since we are interested in control system design, it will also be important to faithfully capture the input-output dynamics of the system. Both of these objectives can be achieved through the use of balanced truncation with an output projection onto a reduced set of dominant POD modes. Indeed, it is well-established that POD modes constitute an optimal reduced basis for approximating the system energy. Further, by treating the associated POD coefficients as system outputs, balanced truncation can be performed to optimally capture the response of POD coefficients to control inputs. A more detailed discussion of these ideas can be found in [23]. Here, we briefly summarize the general ideas surrounding the model reduction procedure.

To compute the POD modes (Φ_r), we first transform the system such that $Q = I$, as described previously. In this new basis, we require the impulse response matrices $G_i(t)$ from the ith input to the full-state output for each of the p inputs. Here, we numerically form a matrix of impulse response data $H := \begin{bmatrix} G_1(t) & G_2(t) & \cdots & G_p(t) \end{bmatrix}$ and perform a singular value decomposition (SVD) of H to determine the dominant POD modes using the snapshot POD method. The leading $r < n$ left singular vectors are stored in a matrix Φ_r, corresponding to the set of r dominant POD modes that optimally capture the system energy. Specifically, we have

$$E(t) \approx \mathbf{z}^T(t)\Phi_r^T \Phi_r \mathbf{z}(t), \tag{6}$$

which is the closest approximation of the energy defined in (2) (recall that POD modes here were computed in a transformed basis such that $Q = I$).

With the POD truncation completed, we next augment the original system in (1) with an output equation that corresponds to the POD coefficients $\mathbf{z}(t)$,

$$\dot{\mathbf{x}}(t) = A\mathbf{x}(t) + B\mathbf{u}(t)$$
$$\mathbf{z}(t) = \Phi_r^T \mathbf{x}(t). \tag{7}$$

At this point, note that the number of outputs is equal to the number of POD modes r that have been retained for energy modeling; however, the state dimension is still $n > r$. We now proceed to perform a balanced truncation of the system in (7) in order to reduce the number of states in the model to $s < n$, while optimally preserving the input-output dynamics.

To do so, we first perform a balancing transformation $\bar{x} = Tx$ such that the controllability Gramian W_c and observability Gramian W_o are equal and diagonal. A truncation can now be performed in this balanced coordinate system, thus allowing the s most controllable and observable modes (i.e., those with relatively large Hankel singular values (HSVs)) to be kept, and the $n - s$ least controllable and observable modes (i.e., those with relatively small HSVs) to be discarded.

The reduced-order system after truncation is of the form:

$$\dot{\bar{\mathbf{x}}}_1 = \bar{A}_{11}\bar{\mathbf{x}}_1 + \bar{B}_1\mathbf{u} \tag{8}$$

$$\mathbf{y} = \bar{C}_1\bar{\mathbf{x}}_1 \tag{9}$$

where $\bar{\mathbf{x}}_1 \in \mathbb{R}^s$, $\bar{A}_{11} \in \mathbb{R}^{s \times s}$, $\bar{B}_1 \in \mathbb{R}^{s \times p}$, and $\bar{C}_1 \in \mathbb{R}^{r \times s}$. In this work, we take the number of states in the reduced-order model to be the same as the number of POD modes used for output projection (i.e., $r = s$); therefore, we will use r to report the order of the reduced model in section III.

III. Results

The linearized channel flow problem has been used as the system model. The controller synthesis approach and the ROM approach described in previous sections have been applied to this model. The channel flow equations are linearized about the laminar solution. After linearization, another approximation of spatial discretization has been performed. The system has been discretized in the stream-wise, span-wise and wall-normal directions, and this is done using the Fourier-Fourier-Chebyshev spectral collocation method. To provide actuation, wall-transpiration using blowing and suction with zero net mass flow is applied at the upper-and lower-walls of the channel. This system uses simultaneous wall normal actuation with the rate of flow as the system input. Full details of this model are outlined in [18].
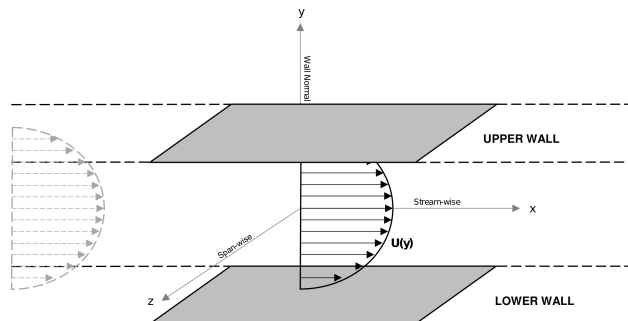

Figure 1: A schematic representation of the channel flow coordinate system.

We investigate the performance of the reduced-order model compared to the full-order model. In this paper, we study the system with stream-wise and span-wise wavenumber pair $(\alpha, \beta) = (1, 0)$. The resulting full-order model has the state dimension $n = 199$. While we study a system using a single set of wavenumber pairs, the Reynolds number (Re) and dimension of the reduced-model (r) are varied to analyze controller performance.

III.A. Reduced-order models

To analyze the performance of the reduced-order modeling approach, we compare the frequency response of the ROM with that of the full-order model (FOM). For multiple-input multiple-output (MIMO) systems, it is common to study the variation of the system's principal gains, which can be used to assess a system's input-output behavior [21]. From the frequency domain analysis, the ROMs seem to reasonably capture the frequency response of the full-order system for $r \geq 6$ at $Re = 1000$, 3000 and $Re = 5000$ (Figure 2).

To better understand the performance of the ROMs, we perform a time-domain analysis by subjecting the system to an arbitrarily constructed input signal that contains multiple frequencies. The results for
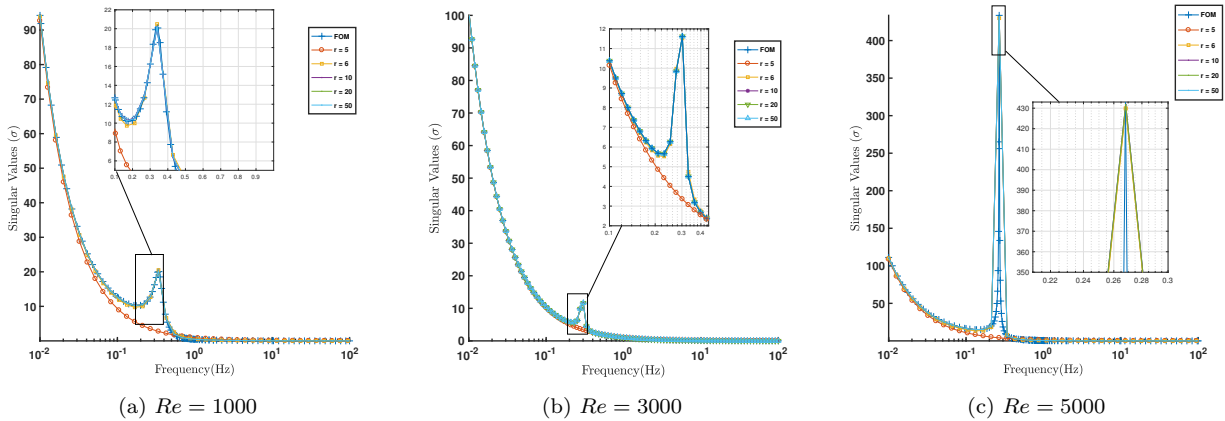
(a) $Re = 1000$ (b) $Re = 3000$ (c) $Re = 5000$

Figure 2: Frequency response of FOM and ROMs shows the singular values over frequencies for 3 different Reynolds number (Re).

the time-domain analysis at $Re = 3000$ are shown in Figure 3. Even though a frequency domain analysis provides a reasonable approximation at high and low frequencies with $r = 6$, we can see in Figure 3 that the model of order $r = 6$ performs poorly to capture the dynamics of the FOM; in contrast, ROMs with $r \geq 10$ capture the time-domain response much better. To better quantify this, we use the root-mean square error (RMSE) between the FOM and ROMs as a metric to evaluate the performance of the reduced-order models performance in the time domain. The RMSE between the FOM and various ROMs is shown in table 1a. It is clear that a higher-order ROM will better approximate the FOM, as is expected.
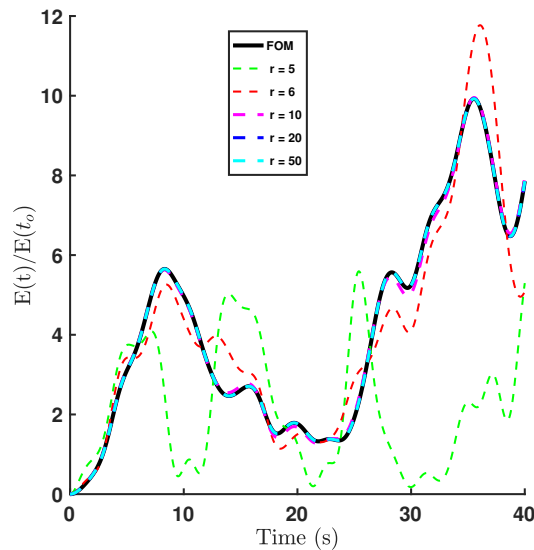

Figure 3: Time domain response of various reduced-order models, when subjected to an arbitrary input signal with multiple frequencies. A reduced-order model of $r \geq 10$ captures the dynamics of the full-order model of dimension $n = 199$. The increase in r enables better capturing the full-model dynamics.

We next compare the HSVs between the ROMs and the FOM (see Figure 4b). In our system, the four dominant input-output modes are associated with the actuator dynamics, but these are not plotted here. We also analyze the contribution of the POD modes in Figure 4a, as POD modes are used in our system to find the closest approximation of energy. It is necessary to capture most of the energy of the system, and thereby an appropriate number of POD modes must be chosen. From the results here, it can be seen that the first 9 POD modes capture $> 96\%$ of the energy; however, it is necessary to have at least 50 POD modes

	$r=5$	$r = 6$	$r = 10$	$r = 20$	$r = 50$
RMS Error	3.6509	0.8222	0.0840	0.0029	8.8797×10^{-6}

Table 1: RMS Error between full-order model and reduced-order model decreases with increase in r. The dimension (n) of the full-order model is $n = 199$ and the $Re = 3000$.

to capture $> 99.99\%$ energy. For the LMI-based synthesis conducted here, it is required that the number of POD modes and the number of balancing modes must be the same (i.e., $r = s$). Thus, the model dimension is dictated by analysis of both the HSV analysis and the cumulative energy analysis.
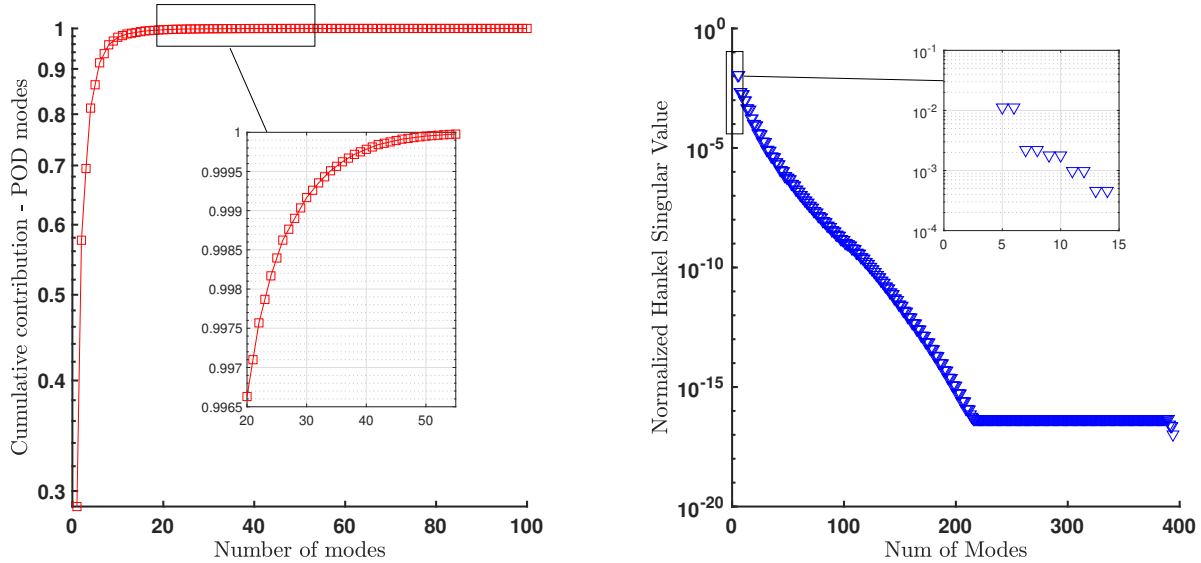
(a) Cumulative energy contribution of each POD mode at $Re = 3000$ & $r = 40$.

(b) Normalized Hankel Singular Values of the system at $Re = 3000$ & $r = 40$.

Figure 4: POD and Hankel Singular Values of the system with $Re = 3000$. (a) 9 POD modes capture $\approx 96\%$ of the energy while 50 modes are essential to capture $\approx 99.99\%$ energy. (b) The Hankel Singular Values (HSV) are normalized by the sum. The HSV shows the contribution of each mode in capturing input-output dynamics.

III.B. Feedback Control

In this section, we use the ROMs from the previous section to design control laws, then implement these controllers and study performance on the FOM. The performance here is reported in terms of the response of energy to an associated optimal disturbance, which is calculated using the methods described in [22]. The controlled response for LQR and LMI-based control for $Re = 3000$ is reported in Figure 5. As r is increased, it is seen that the ROM-based LQR controller quickly starts to approximate the performance of the full-order LQR controller. For the LMI-controller, we see that for $r < 38$, the resulting controller will not outperform LQR controllers developed on the FOM or any ROMs; however, for $r \geq 38$, the ROM-based LMI design reduces the maximum TEG relative to these other control approaches. For $r = 40$, the ROM-based LMI controller reduces the maximum TEG to almost half of that attained by LQR controllers. Note, even at $r = 40$, this significant reduction in the order of system relative to $n = 199$.

For $r = 40$, the 30 dominant eigenvalues of each of the closed-loop systems are plotted alongside the uncontrolled FOM in Figure 6. The uncontrolled system has two poles at zero, which are integrators associated with the actuator dynamics. It can be seen in Figure 6 that the LMI controller mostly alters the spectrum of eigenvalues with real part ≥ -0.5. The closed loop system with LMI and LQR on the full order model place the eigenvalues with real part ≤ -0.6 very close to each other. Comparing the LQR-FOM

(a) $r = 6$ Modes

(b) $r = 10$ Modes

(c) $r = 20$ Modes
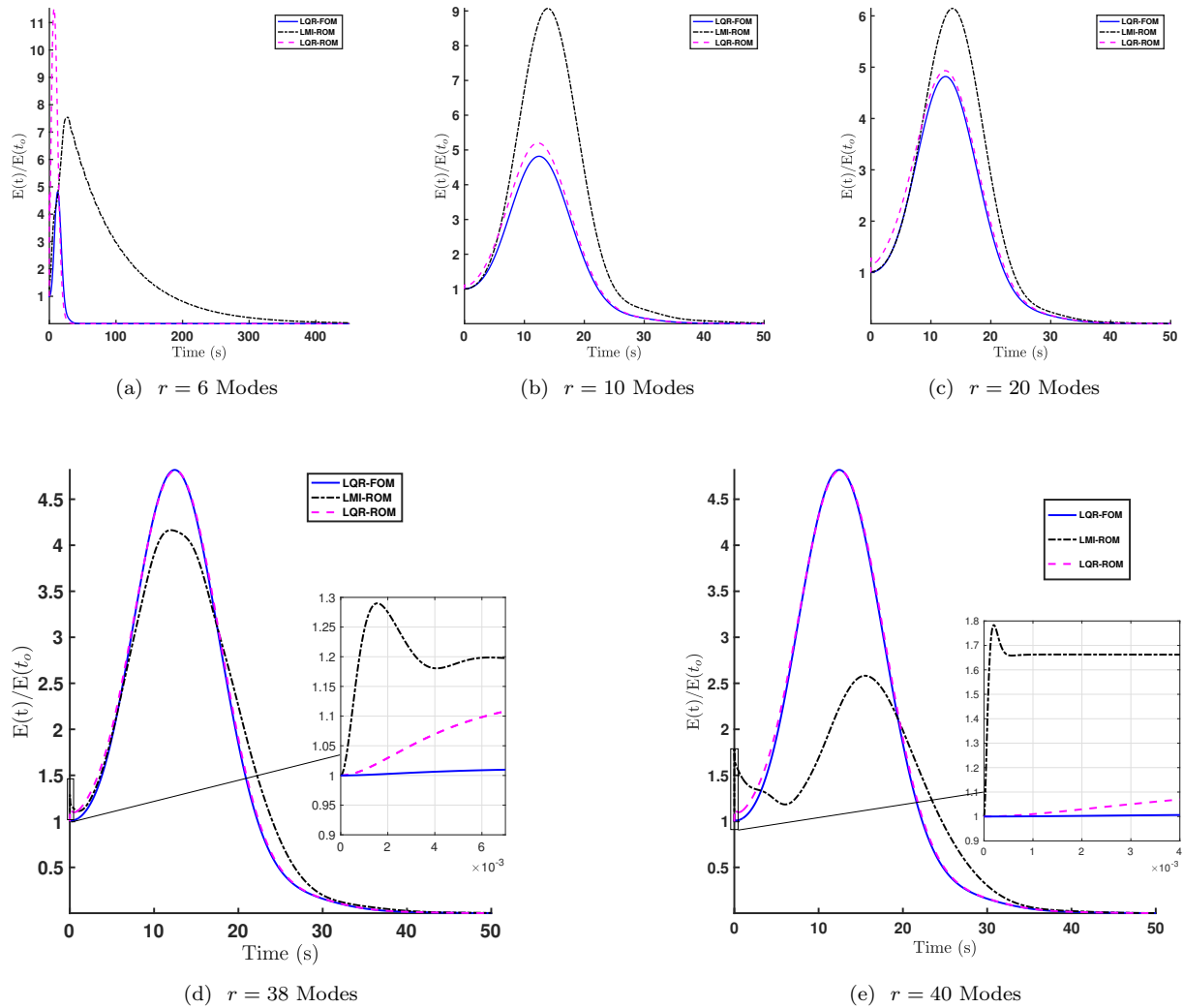
(d) $r = 38$ Modes

(e) $r = 40$ Modes

Figure 5: In figure 5a through 5e, LMI controllers performance in suppressing transient energy growth gets better as the order of the reduced system is increased, while the LQR controller developed on the reduced system starts performing similar to the LQR developed on the full-order model at order approximately $r = 20$. The inset in (c) & (d) shows changes observed in transient energy.

with LQR-ROM eigenvalues reveals a striking similarity, helping to explain the similarity observed in the response of these controlled systems. The streamwise velocity profiles associated with the five dominant modes from each system are reported in Figure 7. It can be seen in Figures 7a through Figure 7e, that the LQR controllers developed on the reduced-order model and full-order model have a very similar performance. In contrast the LMI control yields modes that are dissimilar to both the LQR controllers in various regions along the wall-normal direction, except for in Figure 7a where the LMI control closely resembles the LQR control.

We also performed a robustness assessment of the LMI controller designed for $Re = 3000$. A study was conducted by varying Re by 10%, which was found to cause the LMI controller to destabilize the system. In this respect, both LQR controllers outperformed the LMI controller; they were found to be more robust to parameter uncertainty
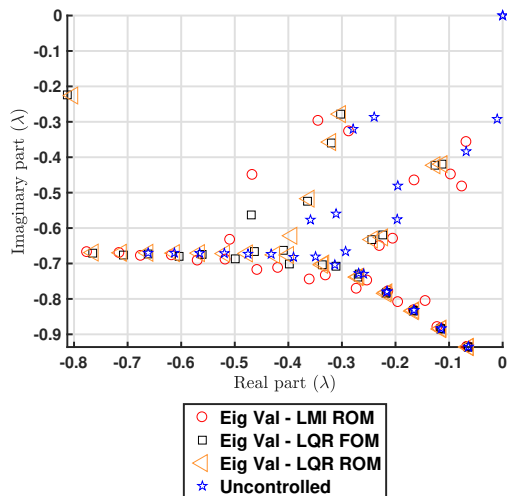
Figure 6: 30 dominant eigenvalues of the uncontrolled and controlled system.

Finally, we conduct controller designs for $Re = 5000$ and $Re = 10000$ (see Figure 8). Note that the $Re = 10000$ case is linearly unstable without control. We find that the model order required to achieve adequate control performance differs between these systems. However, in all cases, LMI-based synthesis using a ROM is able to outperform the LQR-based controllers in terms of reducing TEG.

IV.   Discussion and Conclusion

In this study, we have shown that it is possible to develop controllers to minimize the maximum transient energy growth using ROMs. The ROMs introduced in this paper have been shown to be effective in capturing the input-output response of the original system, while also maintaining a faithful approximation of the system's energy. The use of ROMs for controller synthesis enables us to achieve a superior reduction in TEG relative to linear quadratic designs; however, it should be noted that the ROM-based LMI controllers developed here were found to be sensitive to Re variations, thus lacking desirable robustness properties. This is a disadvantage for flow control since exact models are rare. Future work will need to investigate techniques by which to robustify these controller synthesis techniques.
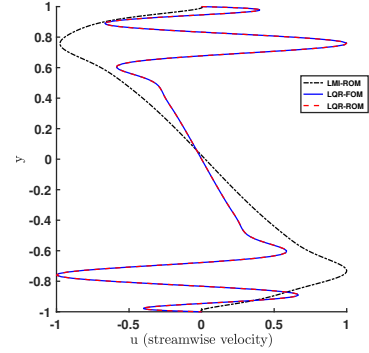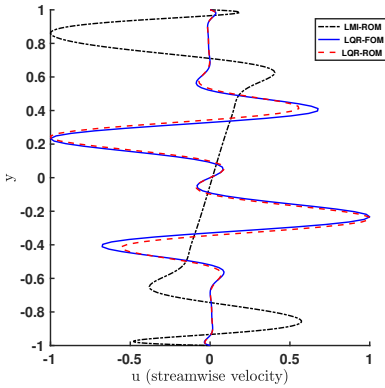
V.   Acknowledgments
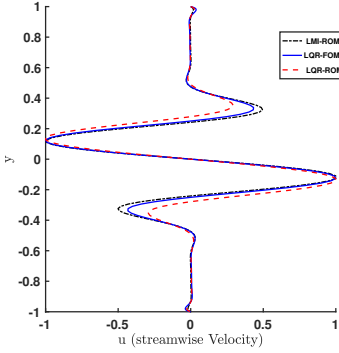
(a) Mode 1: The associated closed loop eigenvalue are $\lambda_{LMI\ ROM} = -0.0639 - i0.935$, $\lambda_{LQR\ ROM} = -0.0640 - i0.9355$ & $\lambda_{LQR\ FOM} = -0.0640 - i0.9355$.
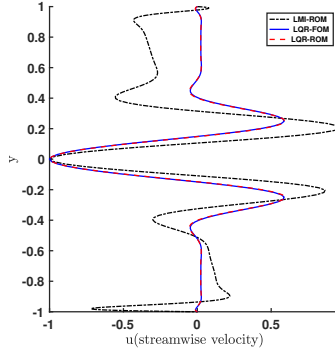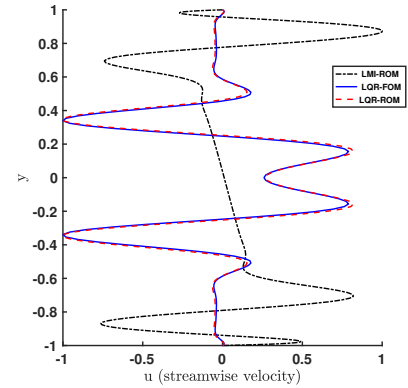
(b) Mode 2: The associated closed loop eigenvalues are: $\lambda_{LMI\ ROM} = -0.0665 - i0.9355$, $\lambda_{LQR\ ROM} = -0.0644 - i0.9359$ & $\lambda_{LQR\ FOM} = -0.0644 - i0.9359$.

(c) Mode 3: The associated closed loop eigenvalues are: $\lambda_{LMI\ ROM} = -0.0676 - i0.3570$, $\lambda_{LQR\ ROM} = -0.1130 - i0.4195$ & $\lambda_{LQR\ FOM} = -0.1131 - i0.4195$.
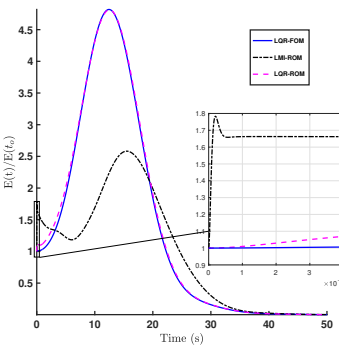
(d) Mode4: The associated closed loop eigenvalues are: $\lambda_{LMI\ ROM} = -0.0757 - i0.4826$, $\lambda_{LQR\ ROM} = -0.1149 - i0.8839$ & $\lambda_{LQR\ FOM} = -0.1149 - i0.8839$.
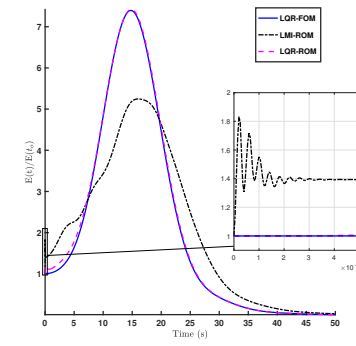
(e) Mode 5: The associated closed loop eigenvalues are: $\lambda_{LMI\ ROM} = -0.0966 - i0.4487$, $\lambda_{LQR\ ROM} = -0.1155 - i0.8852$ & $\lambda_{LQR\ FOM} = -0.1149 - i0.8839$.
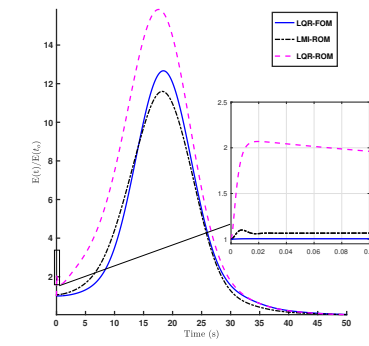
Figure 7: Real part of 5 most dominant eigenvectors for $Re = 3000$,$r = 40$ and the associated eigenvalues are listed in the sub-caption.

(a) The controller is implemented on a system with Re of 3000 & $r = 40$.

(b) The controller is implemented on a system with Re of 5000 & $r = 40$.

(c) The controller is implemented on a system with Re of 10000 & $r = 20$.

Figure 8: The LMI controller suppresses transient energy growth effectively in the sub-critical regime while performing slightly better than the full-order LQR and much better than the LQR on reduced-order model in the unstable regime. The inset in (a), (b) & (c) shows changes observed in transient energy.

References

[1] Joslin, R. D., & Miller, D. N. (Eds.). (2009). Fundamentals and Applications of Modern Flow Control. Reston, VA: American Institute of Aeronautics and Astronautics. https://doi.org/10.2514/4.479892

[2] Schmid, P.J. and Henningson, D.S, Stability and Transition in Shear Flows, Springer-Verlag, New York, 2001.

[3] Butler, K.M., and Farrell, B.F., "Three-Dimensional Optimal Perturbations in Viscous Shear Flow," Physics of Fluids, A4, 1992.

[4] Reddy, S.C., and Henningson, D.S., "Energy Growth in Viscous Channel Flows," J. Fluid Mechanics, vol. 252, 1993.

[5] Trefethen, L., Trefethen, A., Reddy, S., and Driscoll, T., "Hydrodynamic Stability without Eigenvalues," Science, vol. 261, 1993.

[6] Joshi, S.S., Speyer, J.L., and Kim, J., "A Systems Theory Approach to Feedback Stabilization of Infinitesimal and Finite-Amplitude Disturbances in Plane Poiseuille Flow," J. Fluid Mechanics, vol. 332, 1997.

[7] Bewley, T.R. and Liu, S., "Optimal and Robust Control and Estimation of Linear Paths to Transition," J. Fluid Mechanics, vol. 365, 1998.

[8] Or, A.C., Speyer, J.L., Kim, J., "Optimal and robust control and estimation of linear paths to transition," J. Fluid Mechanics, vol. 365, 1998.

[9] Kim, J. and Bewley, T.R., "A Linear Systems Approach to Flow Control," Annual Review of Fluid Mechanics, vol. 39, 2007.

[10] McKernan, J., Whidborne, J. F., and Papadakis, G., "Linear Quadratic Control of Plane Poiseuille Flow - The Transient Behavior," International Journal of Control, vol. 80, 2007.

[11] Whidborne, J. F., and McKernan, J., "On the minimization of maximum transient energy growth," IEEE Transactions on Automatic Control, vol. 52, 2007.

[12] Ilak, M. and Rowley, C.W., "Feedback control of transitional channel flow using balanced proper orthogonal decomposition," AIAA Paper 2008-4230, 2008.

[13] Martinelli, F., Quadrio, M., McKernan, J., and Whidborne, J.F., "Linear feedback control of transient energy growth and control performance limitations in subcritical plane Poiseuille flow," Physics of Fluids, vol. 23, 2011.

[14] Boyd, S., Ghaoui E. L., et al, "Linear Matrix Inequalities in System and Control Theory," SIAM

[15] McKernan, J, "Control of Plane Poiseuille Flow: A Theoretical and Computational Investigation,"Ph.D. Thesis " Int. J. on Bifurcation and Chaos, vol 15, 2005

[16] Rowley,C.W.,"Model reduction using proper balanced proper orthogonal decomposition" Int. J. On Bifurcation and Chaos, Vol 15,No 3,2005, pp 997-1013"

[17] Högberg, M., Bewley, T. R., Henningson, D. S. (2003). Linear feedback control and estimation of transition in plane channel flow. Journal of Fluid Mechanics, 481(481), 149–175.

[18] McKernan, J., Papadakis, G., Whidborne, J. F. (2006). A linear state-space representation of plane Poiseuille flow for control design: a tutorial. International Journal of Modelling, Identification and Control, 1(4), 272.

[19] Heinrichs, W. (1989). Improved Condition Number for Spectral Methods. MATHEMATICS OF COMPUTATION, 53(187), 103–119.

[20] Bewley, T. R. (2001). Flow control: New challenges for a new Renaissance. Progress in Aerospace Sciences, 37(1), 21–58.

[21] Skogestad, S., & Postlethwaite, I. (2005). Multivariable feedback control: analysis and design. John Wiley.

[22] Whidborne, J. F., & Amar, N. (2011). Computing the maximum transient energy growth. BIT Numerical Mathematics, 51(2), 447–457.

[23] Rowley, C. W., & Dawson, S. T. M. (2017). Model Reduction for Flow Analysis and Control. Annu. Rev. Fluid Mech, 49, 387–417.

[24] Taira, K., Brunton, S. L., Dawson, S. T. M., Rowley, C. W., Colonius, T., Mckeon, B. J., Ukeiley, L. S. (n.d.). Modal Analysis of Fluid Flows: An Overview.

[25] Schmid, P. J. (2007). Nonmodal Stability Theory. Annu. Rev. Fluid Mech, 39, 129–62.